



Available online at [www.sciencedirect.com](http://www.sciencedirect.com)

ScienceDirect

Journal of Taibah University for Science 10 (2016) 381–385

J<sup>of Taibah University  
for Science  
Journal</sup>

[www.elsevier.com/locate/jtusci](http://www.elsevier.com/locate/jtusci)

# Sintering temperature effect on density, structural and morphological properties of Mg- and Sr-doped ceria

Syed Ismail Ahmad <sup>a,\*</sup>, P. Koteswar Rao <sup>b</sup>, Iizhar Ahmed Syed <sup>c</sup>

<sup>a</sup> Department of Basic Sciences – Physics Division, Ibn Sina National College, Jeddah, Saudi Arabia

<sup>b</sup> Centre for Nano Science and Technology, IST, JNTU Hyderabad, India

<sup>c</sup> Department of Pharmaceutics, Ibn Sina National College, Jeddah, Saudi Arabia

Available online 29 April 2015

## Abstract

Strontium and magnesium doped ceria solid solutions ( $\text{Ce}_{0.99}\text{Sr}_{0.01}\text{O}_{1.995}$  and  $\text{Ce}_{0.99}\text{M}_{0.01}\text{O}_{1.995}$ ) were synthesized by a cost effective solid state reaction. The doped and un-doped  $\text{CeO}_2$  samples were sintered at 1200 °C, 1300 °C and 1400 °C to investigate the effect of sintering temperature and doping on density, structural and morphological properties. The density was measured by Archimedes' method. It is observed that the density increases with increasing sintering temperature and with doping of strontium. The crystal structure and surface morphology have been characterized by X-ray diffraction (XRD) and scanning electron microscopy (SEM). XRD and SEM reveals that the synthesized samples are single phase with a cubic fluorite structure, and the grains formed are of different sizes. The grain size depends on sintering temperature and type of doping. The lattice parameter increases with sintering temperature and substitution of Sr in ceria. The Grain size of Sr-doped ceria decreases, whereas that of Mg-doped ceria increases. EDS spectra show that the samples are free of contaminants. The  $\text{Ce}_{0.99}\text{Sr}_{0.01}\text{O}_{1.995}$  shows a more open structure than un-doped ceria.

© 2015 The Authors. Production and hosting by Elsevier B.V. on behalf of Taibah University. This is an open access article under the CC BY-NC-ND license (<http://creativecommons.org/licenses/by-nc-nd/4.0/>).

**Keywords:** Doped ceria; Relative density; XRD; SEM; EDS; SOFC

## 1. Introduction

Among various types of fuel cells, solid oxide fuel cells (SOFC) have multi-fuel capability, a high

conversion efficiency of approximately 60% and flexibility in their operation. The electrolyte of an SOFC must be dense, have high ionic conductivity and zero electronic conductivity [1,2]. Yttria-stabilized zirconia (YSZ) can be used as an SOFC electrolyte, but the high operating temperature of ~1000 °C necessary for oxygen ion conductivity would decrease the efficiency and stability of the cell [3,4]. Cerium oxide has a peculiar function different from other rare-earth oxides, as it tends to consist of non-stoichiometric compounds with +4 and +3 oxidation states of cerium. The redox property of ceria leads to oxygen vacancies resulting in a very high oxygen ion conductivity when compared with YSZ, even at intermediate temperatures of 600–800 °C. Ceria doped with alkali earth metal oxides such as CaO and SrO

\* Corresponding author at: Basic Sciences Department – Physics Division, Ibn Sina National College, P.O. Box No. 31096, Jeddah 21418, Saudi Arabia. Tel.: +966 568653832/6356555; fax: +966 6375344.

E-mail address: [dr.syedismailahmad@gmail.com](mailto:dr.syedismailahmad@gmail.com) (S.I. Ahmad).  
Peer review under responsibility of Taibah University.



Production and hosting by Elsevier

<http://dx.doi.org/10.1016/j.jtusci.2015.04.003>

1658-3655 © 2015 The Authors. Production and hosting by Elsevier B.V. on behalf of Taibah University. This is an open access article under the CC BY-NC-ND license (<http://creativecommons.org/licenses/by-nc-nd/4.0/>).

has been studied extensively [5–7]. The conductivity of CaO-doped ceria is much greater than calcia-stabilized zirconia (CSZ) [8,9]. Ceria solid solutions with the formula  $\text{Ce}_{1-x}\text{M}_x\text{O}_{2-\delta}$ , where M is a rare earth metal or lanthanide, show more open structures, possess higher oxygen ion conductivities and are potential electrolytes for low temperature SOFCs (LT-SOFC) [10–12]. To achieve high ionic and zero electronic conductivity, an SOFC electrolyte requires high density and low porosity. The open structure of doped cerium oxides have high ionic conductivities and can be synthesized by various routes. The crystal structure and relative density of solid ceria electrolytes increases with increasing sintering temperature [13]. Alkali earth oxides such as MgO, CaO and SrO are soluble in the ceria lattice, and the resultant materials are suitable candidates for the electrolyte in LT-SOFCs. Mechanically mixed powders of CeO<sub>2</sub> and Sm<sub>2</sub>O<sub>3</sub> have been studied extensively [14]. Gadolinium doped ceria (GDC) and samarium doped ceria (SDC) synthesized by the solid state reaction method have been studied extensively for the effects of sintering temperature on density, porosity, structural and electrical properties [15–17]. Ceria co-doped with rare earth and alkali earth metals have also been synthesized by the solid state reaction method. Their densities increased while their porosities decreased with sintering temperature yielding higher oxygen ion conductivities [18,19]. To explore simpler and cheaper synthesis methods for SOFC electrolytes and to study the effect of temperature on un-doped and Mg- and Sr-doped ceria, representative samples were prepared and investigated.

## 2. Experimental

### 2.1. Sample preparation

Commercially available powders of CeO<sub>2</sub>, MgO and SrCO<sub>3</sub> (AR grade, Sigma Aldrich, USA, 99.9% purity) were used as starting materials. The powders of CeO<sub>2</sub> and SrCO<sub>3</sub> were mixed in the appropriate stoichiometric proportions (1 mole%) to make Ce<sub>0.99</sub>Sr<sub>0.01</sub>O<sub>1.995</sub>. The mixture was ground in agate and mortar to obtain a homogenized powder. The powder was calcined at 800 °C for 2 h to decompose the SrCO<sub>3</sub> and reground. Two mole% of polyvinylpyridine was added to the powder as a binder and was mixed thoroughly. The powder sample was uni-axially pressed by a pressure of 10 tons/sq inch to obtain disc-shaped pellets. Ce<sub>0.99</sub>Mg<sub>0.01</sub>O<sub>1.995</sub> and un-doped CeO<sub>2</sub> pellets were prepared in a similar manner. The prepared pellets were sintered at 1200 °C, 1300 °C and 1400 °C for 2 h in air, at a ramp of 2 °C/min and cooled to room temperature

by the rate. The prepared un-doped CeO<sub>2</sub> pellets were identified as CE12, CE13 and CE14; Sr-doped pellets as SC12, SC13 and SC14; and Mg-doped pellets as MC12, MC13 and MC14, which were sintered at temperatures of 1200 °C, 1300 °C and 1400 °C, respectively. Additionally, bulk densities ( $d_B$ ) were determined for the aforementioned samples. Finally, a total of six dense pellets (CE12, CE13 and CE14, Sr-doped pellets SC13 and SC14 and Mg-doped MC14) were used for characterization.

## 2.2. Characterization

### 2.2.1. Density

Bulk densities ( $d_B$ ) of the sintered samples were measured by Archimedes' method. The theoretical densities were measured by the formula

$$d_{th} = \frac{4}{A^3 N_a} [0.99M_C + 0.01M + 1.995M_O] \quad (1)$$

where M<sub>C</sub>, M<sub>O</sub> and 'M' are atomic wt. of ceria; oxygen and the dopants Sr and Mg; and A is the lattice parameter.

### 2.2.2. Structure and morphology

The phase and structural properties of sintered pellets were studied by powder X-ray diffraction (XRD) using Cu K $\alpha$  radiation ( $\lambda = 1.54 \text{ \AA}$ ) as the radiation source at 40 kV and 30 mA. The crystalline size 'D' was measured by Scherrer's formula

$$D = \frac{0.94\lambda}{\beta \cos \theta} \quad (2)$$

where  $\beta$  is FWHM of the peak and  $\theta$  is Bragg angle. The lattice parameter was calculated by using the relation

$$a = d\sqrt{h^2 + k^2 + l^2} \quad (3)$$

Surface morphology was characterized by scanning electron microscopy (ZEISS Evo series SEM) at an operating voltage of 15 kV. Grain size was measured from higher magnification SEM micrographs.

## 3. Results and discussion

The measured bulk densities,  $d_B$ , of samples are between 86% and 94% of their theoretical densities,  $d_{th}$ . Table 1 gives the relative densities of samples sintered at different temperatures. It is observed that the relative density increases with increasing sintering temperature, as shown in Fig. 1.

Substitution of Sr in ceria leads to an increase in density of the ceria solid solution. The relative density is

Table 1  
Sample identification and densities.

S.no.	Sample code	Temperature (°C)	Composition	$d_m$ (g/cc)	$d_{th}$ (g/cc)	%Relative density
1	CE12	1200	CeO <sub>2</sub>	6.199 ± 0.047	7.221	86
2	CE13	1300	CeO <sub>2</sub>	6.467 ± 0.021	7.209	90
3	CE14	1400	CeO <sub>2</sub>	6.680 ± 0.022	7.186	93
4	SC13	1300	Ce <sub>0.99</sub> Sr <sub>0.01</sub> O <sub>1.995</sub>	6.479 ± 0.021	7.120	91
5	SC14	1400	Ce <sub>0.99</sub> Sr <sub>0.01</sub> O <sub>1.995</sub>	6.591 ± 0.027	7.013	94
6	MC14	1400	Ce <sub>0.99</sub> Mg <sub>0.01</sub> O <sub>1.995</sub>	6.550 ± 0.021	7.122	92

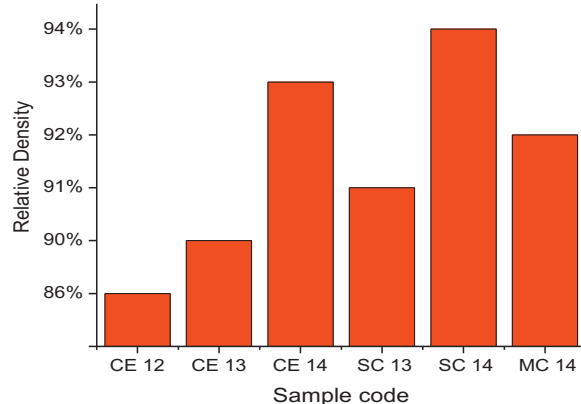


Fig. 1. Relative density vs sintering temperature.

approximately 93% of the theoretical density at temperature 1400 °C for ceria and 94% for strontium doped ceria. The substitution and increase in the content of Sr in ceria [10,20] and Gd in ceria [21] increases its density. However, in the case of Mg-doped ceria, no great change in density has been observed, probably because of its size mismatch and lesser atomic wt.

The X-ray diffraction patterns obtained for CE12, CE13 and CE14 are shown in Fig. 2, and diffraction patterns for CE14, SC13, SC14 and MC14 are shown in Fig. 3. All of the samples are single phase. The results are compared with JCPDS card no. 81-0792. The

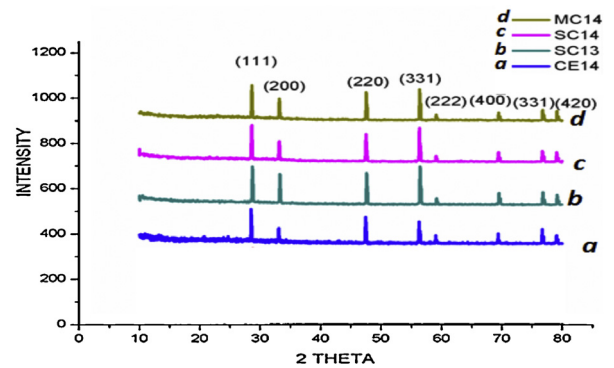


Fig. 3. X-ray diffraction pattern of CE14, SC13, SC14 and MC14.

samples show the presence of (1 1 1), (2 0 0), (2 2 0), (3 1 1), (2 2 2), (4 0 0) and (3 3 1) diffraction peaks in the scanning range of  $2\theta = 20\text{--}90^\circ$ , and exhibit cubic fluorite structure. The crystalline size and lattice parameters were calculated using Eqs. (2) and (3). Table 2 gives lattice parameters for the samples sintered at different temperatures. It is evident from Fig. 2 that as the sintering temperature increases the (1 1 1) diffraction peak shifts towards a lower value of  $2\theta$  [22]. Lattice parameters increase linearly with increasing temperature [13,23]. Deviation of the lattice parameter,  $\Delta a$  ( $\Delta a = |a_{CE} - a_{doped}|$ ) from un-doped ceria CE14 was found at a maximum (0.008) for CS14 and at a minimum

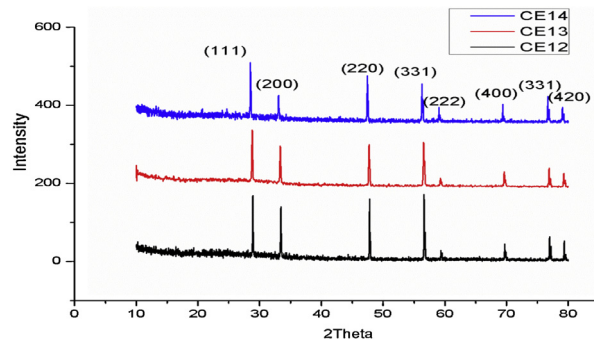


Fig. 2. X-ray diffraction pattern of un-doped ceria at different temperatures.

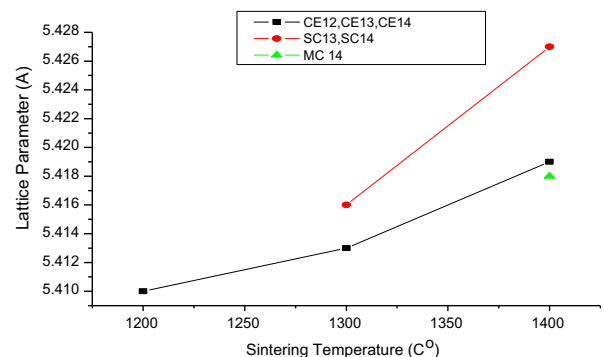


Fig. 4. Lattice parameter vs sintering temperature.

Table 2  
Results of XRD and SEM.

S.no.	Sample	Crystallite size (nm)	Lattice parameter (Å)	Grain size (μm)
1	CE12	19.3	5.410	5.9
2	CE13	24.93	5.413	5.7
3	CE14	29.08	5.419	5.5
4	SC13	19.15	5.416	3.8
5	SC14	24.08	5.427	3.0
6	MC14	21.11	5.417	6.3

for MC14 as shown in Fig. 4. A range in crystal size from 19.3 to 29.08 nm is observed.

From Fig. 3, it is clear that the peaks corresponding to doped samples shifted to lower  $2\theta$  values, which indicates an increase in the lattice parameter. As shown in Table 2, the lattice parameters of SC13 and SC14 are greater than that of CE13 and CE14. This could be attributed to the difference in size of the two metal atoms with the size of  $\text{Ce}^{+4}$  (0.97 Å) being less than that of  $\text{Sr}^{+2}$  (1.21 Å) [15,19,24]. Whenever a material is doped with a dopant of higher atomic radii ( $r_d > r$ ) the diffraction peak maximum shifts towards a lower value of  $2\theta$ ; conversely, it shifts to a higher  $2\theta$  value when  $r_d < r$  [20,22,25]. In the present study, the (1 1 1) peak of

MC14 shifts towards the right when compared with that of CE14, as  $r_{\text{Mg}}$  (0.72 Å)  $< r_{\text{Ce}}$  (0.96 Å).

Micro structures of the sintered pellets are shown in Fig. 5. No pores are observed in high temperature sintered samples, which is consistent with their measured densities. The linear intercept method is applied and higher magnification micrographs are used to measure grain sizes. The grains observed are of varying size. The average grain size for CE14 is 5.5 μm, and that of SC14 is 3 μm. It is evident that the substitution of Sr into the Ceria lattice decreases the grain size, which may be due to the mismatch of size of atomic radii of  $\text{Ce}^{+4}$  and  $\text{Sr}^{+2}$ . However, in the case of Mg-doped ceria the grain size (6.3 μm) increases, which could be

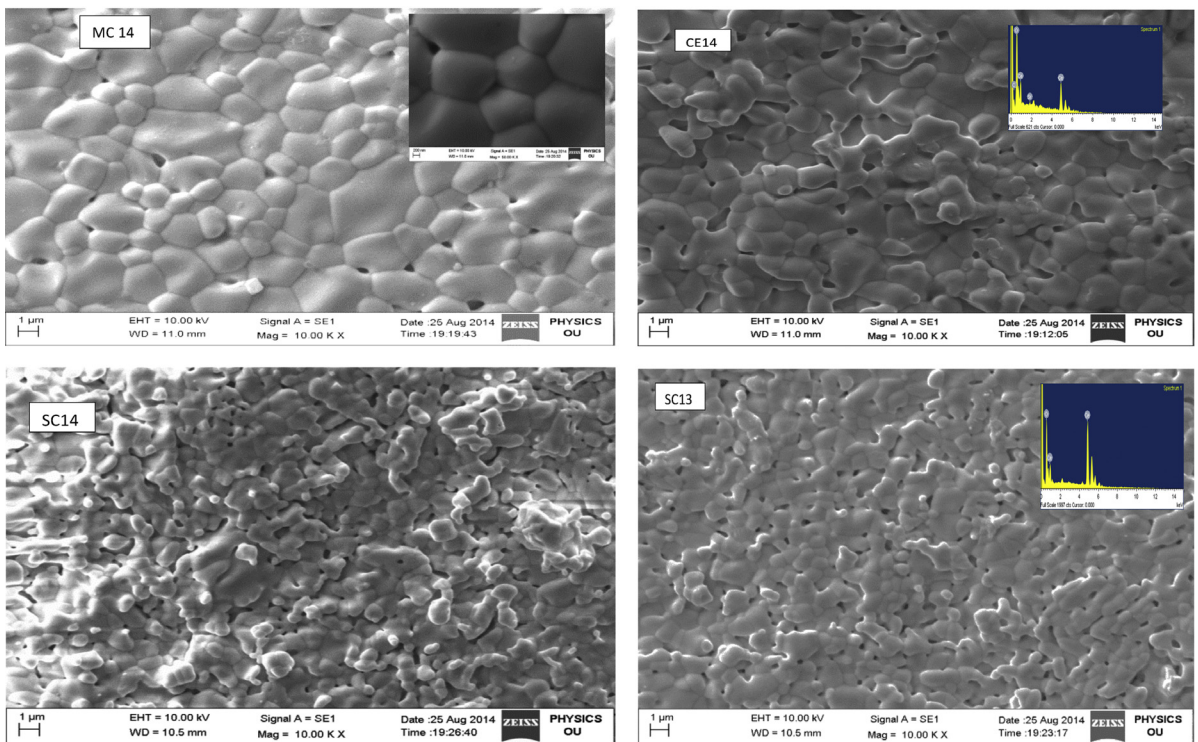


Fig. 5. Scanning electron micrograph (SEM) of doped ceria samples.

due to  $r_{\text{Mg}}$  (0.72 Å)  $<$   $r_{\text{Ce}}$  (0.96 Å). However, as sintering temperature increases, an increment in the grain size is observed.

#### 4. Conclusion

The sintering and doping of Sr and Mg in ceria leads to a change in density, lattice parameter and grain size. The density and lattice parameters of un-doped ceria, Sr-doped and Mg-doped ceria increase with sintering temperature. The alkali earth metals can be used as a sintering aid in ceria. XRD analysis reveals that the lattice parameter increases with sintering temperature and doping. The grain size of cerium oxide decreases with the doping of Sr, giving a more open structure that could exhibit high ionic conductivity.

#### References

- [1] N.Q. Minh, T. Takahashi, *Science and Technology of Ceramic Fuel Cells*, Elsevier, 1995, ISBN 978-0-444-89568-4.
- [2] R. Bove, Solid oxide fuel cells: principles, design and state of the art in industries, in: S. Basu (Ed.), *Recent Trends in Fuel Cell Science and Technology*, Springer and Anamaya Publishers, New Delhi, India, 2007, ISBN 0 387 35537 5 (Chapter 11).
- [3] H. Inaba, H. Tagawa, Ceria-based solid electrolytes: review, *Solid State Ionics* 83 (1996) 1–16.
- [4] M. Biswas, P. Kumar Ojha, E. Moses Jaysingh, C. Durga Prasad, Synthesis of nano crystalline yttria stabilized zirconia for SOFC, *Nanomater. Nanotechnol.* 2 (2011) 55–58.
- [5] O. Poh Shing, Mechanical synthesis and characterization of calcia doped ceria oxide ion conductor, *Mater. Sci. Eng.* 17 (2011).
- [6] K. Yamashita, Hydrothermal synthesis and low temperature conduction properties of substituted ceria ceramic, *Solid State Ionics* 81 (1995) 53–60.
- [7] S. Banerjee, P.S. Devi, Understanding the effect of calcium on the properties of ceria prepared by a mixed fuel process, *Solid State Ionics* 179 (2008) 661–669.
- [8] V.V. Kharton, F.M. Figueirido, L. Lavorro, E.N. Naumovich, Ceria based materials for solid oxide fuel cells, *J. Mater. Sci.* 36 (2001) 1105–1117.
- [9] H. Arai, Electrical properties of calcia-doped ceria with oxygen ion conduction, *Solid State Ionics* 20 (4) (1986) 241–248.
- [10] N. Jaiswal, D. Kumar, S. Upadhyay, Ceria doped with calcium and strontium (Sr): a potential candidate for intermediate temperature fuel cell, *Ionics* 20 (2014) 45–54.
- [11] C. Veranitisagul, A. Kaewvilai, W. Wattanathana, N. Koonsaeng, A. Laobuthee, Electrolyte materials for solid oxide fuel cells derived from metal complexes: gadolinia doped ceria, *Ceram. Int.* 38 (2012) 2403–2409.
- [12] M. Dudek, Ceramic electrolyte in  $\text{Ce}_{0.8-x}\text{Gd}_x\text{O}_3\text{SrO}$  system – preparation, properties and application for solid oxide fuel cells, *Int. J. Electrochem. Sci.* 7 (2012) 2874–2889.
- [13] M.G. Chourasia, J.Y. Patil, S.H. Pawar, L.D. Jadhav, Studies on structural, morphological and electrical properties of  $\text{Ce}_{1-x}\text{Gd}_x\text{O}_{2-x/2}$ , *Mater. Chem. Phys.* 109 (2008) 39–44.
- [14] H. Yahiro, Y. Eguchi, K. Eguchi, H. Arai, Oxygen ionic conductivity of ceria-samarium oxide system with fluorite structure, *J. Appl. Electrochem.* 18 (1998) 527–531.
- [15] L.D. Jadhav, S.H. Pawar, M.G. Chourashiya, Effect of sintering temperature on structural and electrical properties of gadolinium doped ceria ( $\text{Ce}_{0.9}\text{Gd}_{0.1}\text{O}_{1.95}$ ), *Bull. Mater. Sci.* 30 (2007) 97–100.
- [16] M. Buchi Suresh, J. Roy, The effect of strontium doping on densification and electrical properties of  $\text{Ce}_{0.8}\text{Gd}_{0.2}\text{O}_{2-\delta}$  electrolyte for IT-SOFC applications, *Ionics* 18 (2012) 291–297.
- [17] T.-H. Yeh, C.-C. Chou, Ionic conductivity investigation in samarium and strontium co-doped ceria system, *Phys. Scr.* T129 (2007).
- [18] Y. Zheng, S. He, L. Ge, M. Zhou, H. Chen, L. Guo, Effect of Sr on Sm-doped ceria electrolyte, *Int. J. Hydrogen Energy* 36 (2011) 5128–5135.
- [19] S. Ramesh, K.C. James Raju, Structural and ionic conductivity studies of doped ceria electrolyte, *Electrochim. Solid-State Lett.* 15 (2011) B24–B26.
- [20] N. Jaiswal, D. Kumar, S. Upadhyay, O. Prakash, Effect of Mg and Sr co-doping on the electrical properties of ceria-based electrolyte material for intermediate temperature solid oxide fuel cells, *J. Alloys Compd.* 577 (2013) 456–462.
- [21] Y. Ma, Ceria based Nanostructural Material for Low Temperature Solid Oxide Fuel Cells (Dissertation PhD thesis), Royal Institute of Technology, KTH, Stockholm, 2012.
- [22] E.Y. Pikalova,  $\text{CeO}_2$  based materials doped with lanthanides for applications in intermediate temperature electrochemical cell devices, *Int. J. Hydrogen Energy* 36 (2011) 6138–6157.
- [23] S. Ramesh, K.C. James Raju, C. Vishnuvardhan Reddy, Synthesis and characterization of co-doped ceria ceramic by sol-gel method, *Trans. Ind. Ceram. Sci.* 70 (2011) 143–147.
- [24] F.-Y. Wang, S. Chen, Q. Wang, S. Yu, S. Cheng, Study of Gd and Mg Co-doped ceria electrolyte for intermediate temperature solid oxide fuel cell, *Catal. Today* 97 (2004) 189–194.
- [25] H. Zou, Y.S. Lin, N. Rane, T. He, Synthesis and characterization of nanosized ceria powders and high-concentration ceria sols, *Ind. Eng. Chem. Res.* 43 (2004) 3019–3025.